

# Chimeras and solitary states in 3D oscillator networks with inertia

V. Maistrenko<sup>1</sup>, O. Sudakov<sup>1,2</sup>, O. Osiv<sup>1</sup>

<sup>1</sup>*Scientific Center for Medical and Biotechnical Research,  
NAS of Ukraine, 54, Volodymyrs'ka Str., Kyiv 01030, Ukraine*

<sup>2</sup>*Taras Shevchenko National University of Kyiv, 60, Volodymyrs'ka Str., Kyiv 01030, Ukraine*

We report the diversity of scroll wave chimeras in the three-dimensional (3D) Kuramoto model with inertia for  $N^3$  identical phase oscillators placed in a unit 3D cube with periodic boundary conditions. In the considered model with inertia, we have found patterns which do not exist in this system without inertia. In particular, a scroll ring chimera is obtained from random initial conditions. In contrast to this system without inertia, where all chimera states have incoherent inner parts, these states can have partially coherent or fully coherent inner parts as exemplified by a scroll ring chimera. Solitary states exist in the considered model as separate states or can coexist with scroll wave chimeras in the oscillatory space. We also propose a method of construction of 3D images using solitary states as solutions of the 3D Kuramoto model with inertia.

**Chimera states as a phenomenon of coexistence of coherence and incoherence patterns are well known in nonlinear science. This phenomenon appears in models that describe the basic properties of a collective dynamics in various real physical systems. In our study within 3D oscillatory networks with inertia, we investigate the appearance of chimeras and analyze their properties by the example of a scroll ring chimera obtained from random initial conditions. Our results show that, due to the introduction of the inertia, the 3D chimeras are stable despite perturbations of the initial conditions and can be surrounded by solitary oscillators.**

Chimera states [1–3] as a dynamical phenomenon in arrays of non-locally coupled oscillators, that displays a spatio-temporal pattern of co-existing coherence and incoherence, have been elaborately investigated during the past decade in a wide range of systems.

A number of illustrious articles are devoted to the theoretical and experimental studies of chimeras. Most of them deal with *one-dimensional* models. Nonetheless, this novel approach was extended to the *two-dimensional* networks of oscillators. Among other factors, a new class

of chimera states called the spiral wave chimeras has been introduced in [4]. This kind of spatio-temporal behavior is characterized by the standard 2D spiraling and, moreover, by a finite-size incoherent core (see, e.g., [5–14]).

As for the 3D case, we mention a few papers about chimera states in the model of coupled phase oscillators in a *three-dimensional* grid topology [15–20]. The first evidence of chimera states in 3D was reported in 2015 in [15] for the Kuramoto model of coupled phase oscillators in a 3D grid topology with piecewise constant oscillator's coupling. Just this kind of coupling produces a rich variety of chimera states in the 1D Kuramoto model with respect to cosine and exponential couplings [21]. In [15] the 3D oscillating chimera states, i.e., those with no spiraling of the coherent region (incoherent and coherent balls, tubes, crosses, layers), and spiral-shaped rotating chimeras called *scroll wave chimeras* including incoherent rolls of different modalities in the coherent spiral arms were obtained. Some time later, two new kinds of scroll wave chimeras, Hopf link and trefoil, with linked and knotted incoherent regions were detected in [16]. The theoretical confirmation of the existence of a few kinds of 3D chimera states in the Kuramoto model with the cosine coupling of oscillators was done in 2019 in [20].

In the present paper, we study the appearance of 3D chimera states in the Kuramoto model of coupled phase oscillators in the 3D grid topology with inertia:

$$m\ddot{\varphi}_{ijk} + \epsilon\dot{\varphi}_{ijk} = \frac{\mu}{|B_P(i, j, k)|} \sum_{(i', j', k') \in B_P(i, j, k)} \sin(\varphi_{i'j'k'} - \varphi_{ijk} - \alpha), \quad (1)$$

where  $i, j, k = 1, \dots, N$ ,  $\varphi_{ijk}$  are phase variables, and indices  $i, j, k$  are periodic modulo  $N$ . The coupling is assumed long-ranged and isotropic: each oscillator  $\varphi_{ijk}$  is coupled with equal strength  $\mu$  to all its nearest neighbors  $\varphi_{i'j'k'}$  within a ball of radius  $P$ , i.e., to those falling in the neighborhood

$$B_P(i, j, k) := \{(i', j', k') : (i' - i)^2 + (j' - j)^2 + (k' - k)^2 \leq P^2\},$$

where the distances are calculated taking into account

the periodic boundary conditions of the network. The phase lag parameter  $\alpha$  is selected from the range  $[0, \pi/2]$ . The relative coupling radius  $r = P/N$ , varies from  $1/N$  (local coupling) to 0.5 (close to the global coupling).

The parameter  $\mu$  is the oscillator coupling strength, and  $\epsilon$  is the damping coefficient. The parameter  $m$  is the mass. In the case  $m = 0$ , Eq. (1) is transformed into the pure 3D Kuramoto model without inertia. We put  $m = 1$  without any loss of generality.

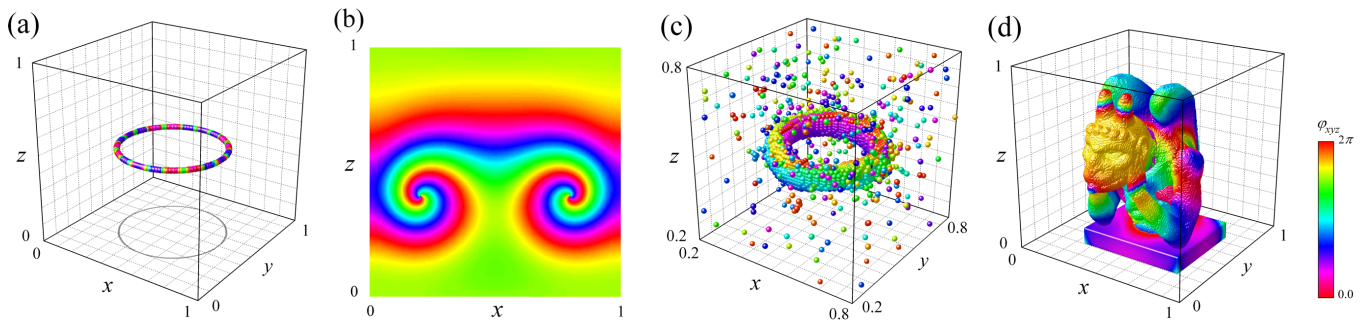


FIG. 1. Phase snapshots of patterns in model (1): (a) - scroll ring, (b) - cross-sections of (a) at  $y = 0.5$  ( $\alpha = 0.38, \mu = 0.02, r = 0.01, N = 200$ ), (c) - scroll ring with solitary cloud ( $\alpha = 0.4, \mu = 0.1, r = 0.04, N = 100$ ), (d) - 3D image of a chimera sculpture generated by solitary states ( $\alpha = 0.35, \mu = 0.1, r = 0.15, N = 200$ );  $\epsilon = 0.05$ . Coordinates  $x = i/N, y = j/N, z = k/N$ .

We study the appearance of a variety of scroll wave chimeras which do not exist in the model without inertia. Their properties are analyzed through the example of scroll ring chimera states (Fig. 1(a,b)). The scroll wave chimera obtained from random initial conditions looks like a mis-shapen scroll ring (Fig. 2) and will be referred hereinafter as a *scroll ring chimera state* [16, 22–24].

Scroll wave chimera states in system (1) without inertia for piecewise constant oscillator’s coupling always have incoherent inner parts [15–17]. In contrast, the scroll wave chimera in system (1) with inertia can have partially coherent or fully coherent inner parts. The diversity of scroll wave chimeras and the impact of inertia on scroll wave chimeras in a system without inertia are analyzed.

We demonstrate that the 3D scroll wave chimeras can be surrounded by solitary oscillators [25, 26] (like a “solitary cloud”) (Fig. 1 (c)). In [27], the spiral wave chimeras with solitary clouds have been studied in the case of the 2D Kuramoto model with inertia.

Finally we propose a method of construction of 3D images using solitary states as solutions of the inertial system (1). An example of a chimera sculpture from the Notre-Dame Cathedral is shown in Fig. 1(d).

Numerical simulations were performed on the base of the Runge–Kutta solver DOPRI5 on a computer cluster CHIMERA, <http://nll.biomed.kiev.ua/cluster>, with graphics processing units [28, 29]. Trajectories were computed and analyzed for system (1) with  $N = 50, 100, 200$  (0.125, 1, 8 mln oscillators, respectively). Coupling radius  $P$  was selected from the range [1, 50]. The random initial conditions were chosen from the phase range  $[0, 2\pi]$  and the frequency range  $[-\mu/\epsilon, \mu/\epsilon]$ , independently for each oscillator.

During the simulation of Eq. (1) without inertia ( $m = 0$ ), we typically observed a birth of scroll ring chimeras from random initial conditions. But in all such cases, the scroll ring appears to be unstable and is destroyed rather rapidly after the start of a simulation. A similar phenomenon was reported in [16].

In the case of the model with inertia ( $m = 1$ ), the random initial condition generates a stable scroll ring chimera which survives, as far as we simulate in time till  $t = 10^5$  with the parameter values  $\alpha = 0.2, r = 0.03, \mu = 0.1, \epsilon = 0.05, N = 100$ .

Figure 2 (Multimedia view) illustrates the time evolution of the random trajectory. At the time  $t \approx 2500$ , two scroll rings have been generated by the random chaotic behavior of oscillators. They exist during the time interval  $t \approx (2500 - 3900)$  (Fig. 2 (a)). Then one ring shrinks and disappears, leading to homogeneous oscillations, but the second ring still survives (Fig. 2 (b)), as far as we simulated (till  $10^5$  time units), and is fixed in the oscillator space. Its cross-section along  $y = 0.5$  is presented in Fig. 2(c).

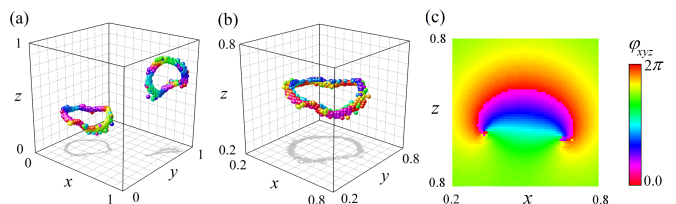


FIG. 2. Generated scroll ring chimera state from random initial conditions. Phase snapshots at  $t = 2500$  (a),  $t = 4000$  (b), cross-section of (b) along  $y = 0.5$  (c). Parameters  $\alpha = 0.2, r = 0.03, \mu = 0.1, \epsilon = 0.05, N = 100$ . Coordinates  $x = i/N, y = j/N, z = k/N$ . (Multimedia view).

Other patterns in model (1) were detected from random initial condition as well. The pattern is considered stable, if it remained stationary for more than 1000 time units. After identifying these patterns, the parameter region for their existence was explored by the standard continuation method with changing parameter values.

In Fig. 3, the parameter regions for a scroll ring chimera and for a few other patterns in  $(\alpha, \mu)$  (a) and  $(\alpha, r)$  (b) parameter planes are presented. The blue region in Fig. 3(a) corresponds to the scroll ring chimera with incoherent or partially coherent inner part, red - scroll ring with completely coherent inner part. The stability region for solitary states, which are considered in detail below, is hatched by gray. Typical shapes of the chimera states are shown in insets. As our simulation shows, the scroll ring chimera states exist for any infinitely small coupling strength  $\mu > 0$ . Crossing the left and left bottom sides of the scroll ring stability region, all oscillators are synchronized. Figure 3(b) also illustrates the parameter regions, but in  $(\alpha, r)$  parameter plane with additional regions for a sphere or ball (green) and 4 scroll wave rods (magenta). Here, the lower bound of the scroll

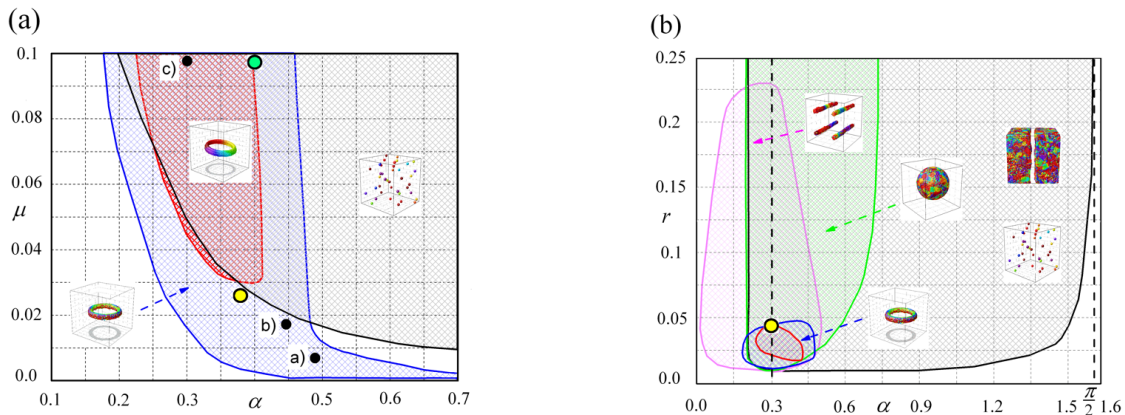


FIG. 3. Parameter regions for chimeras and solitary states in the parameter planes: (a) -  $(\alpha, \mu)$  ( $r = 0.04$ ), (b) -  $(\alpha, r)$  ( $\mu = 0.1$ ). Blue - scroll ring with incoherent or partially coherent inner parts, red - coherent ring, green - sphere, magenta - 4 scroll wave rods, gray - solitary states. Snapshots of typical states are shown in the insets.  $\epsilon = 0.05$ ,  $N = 100$ .

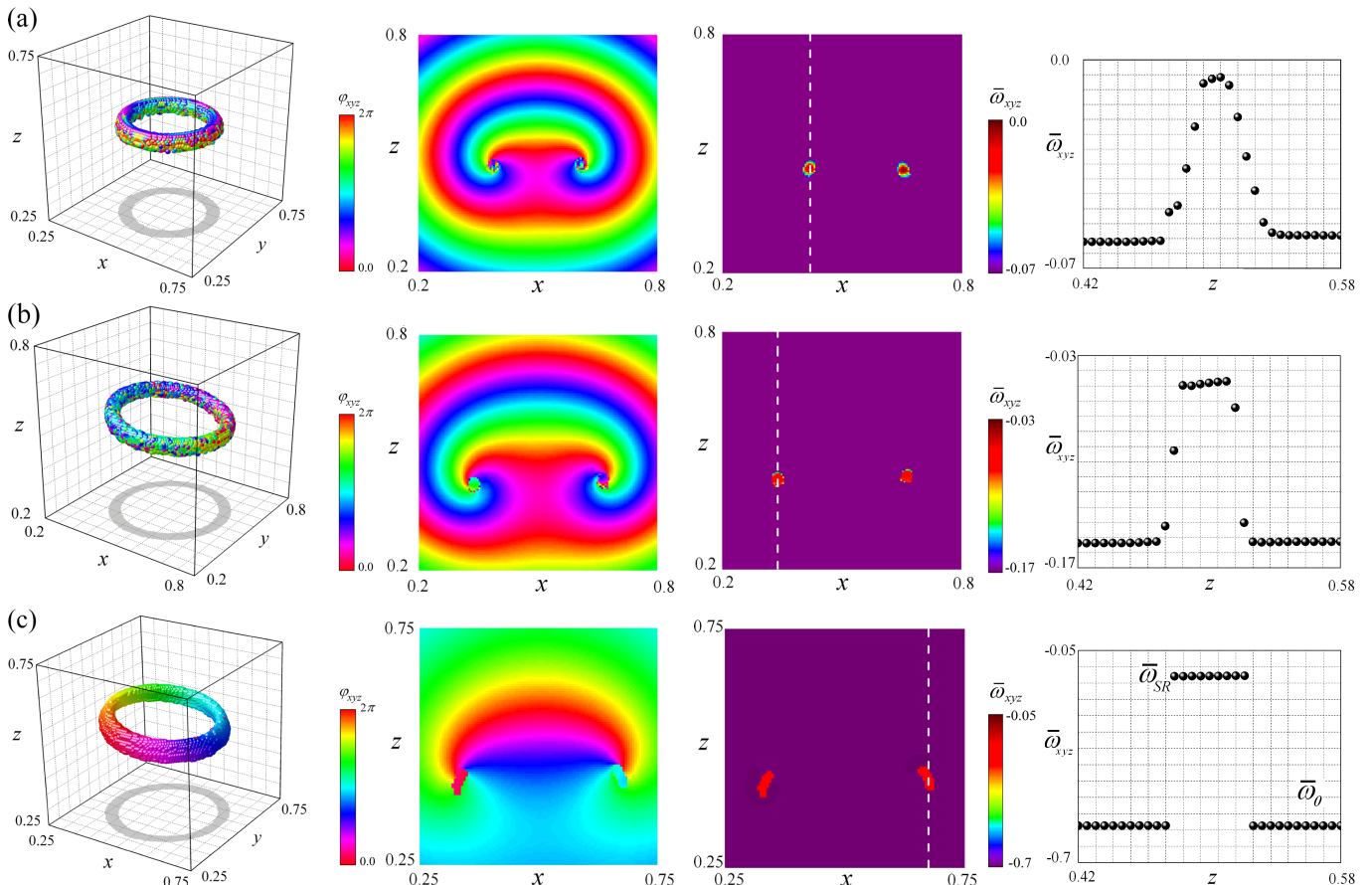


FIG. 4. Examples of scroll ring chimeras. Left column - phase snapshots, next two columns - cross-sections of the phase and average frequencies at the centers of the scroll rings, right column - double cross-sections of average frequencies along the white dashed line on the previous column. (a) - incoherent scroll ring chimera ( $\alpha = 0.475$ ,  $\mu = 0.007$ ) (Multimedia view), (b) - scroll ring chimera with partially coherent inner part ( $\alpha = 0.436$ ,  $\mu = 0.019$ ); (c) - coherent scroll ring. Parameters  $r = 0.04$ ,  $\epsilon = 0.05$ ,  $N = 200$ . Simulation time  $t = 10^4$ . Frequency averaging interval  $\Delta T = 1000$ .

ring region starts from the coupling radius  $P = 1$  (local coupling). Crossing the left and bottom sides of this region, all oscillators are synchronized, and the ring is vanished. After crossing the right side of the region, the rings are destroyed with the generation of the chaotic oscillatory behavior.

Our simulations demonstrate that though Fig. 3 is obtained for model (1) with  $N = 100$ , but similar pa-

parameter regions exist for larger  $N = 200$  and the same relative coupling radius  $r = P/N$ .

The examples of scroll ring chimeras with incoherent, partially coherent, and completely coherent inner parts are presented in Fig. 4. Location of parameter values for the examples are indicated by black points in Fig. 3(a). The average frequency profile of an incoherent scroll ring in Fig. 4(a) (Multimedia view) is smooth and bell-

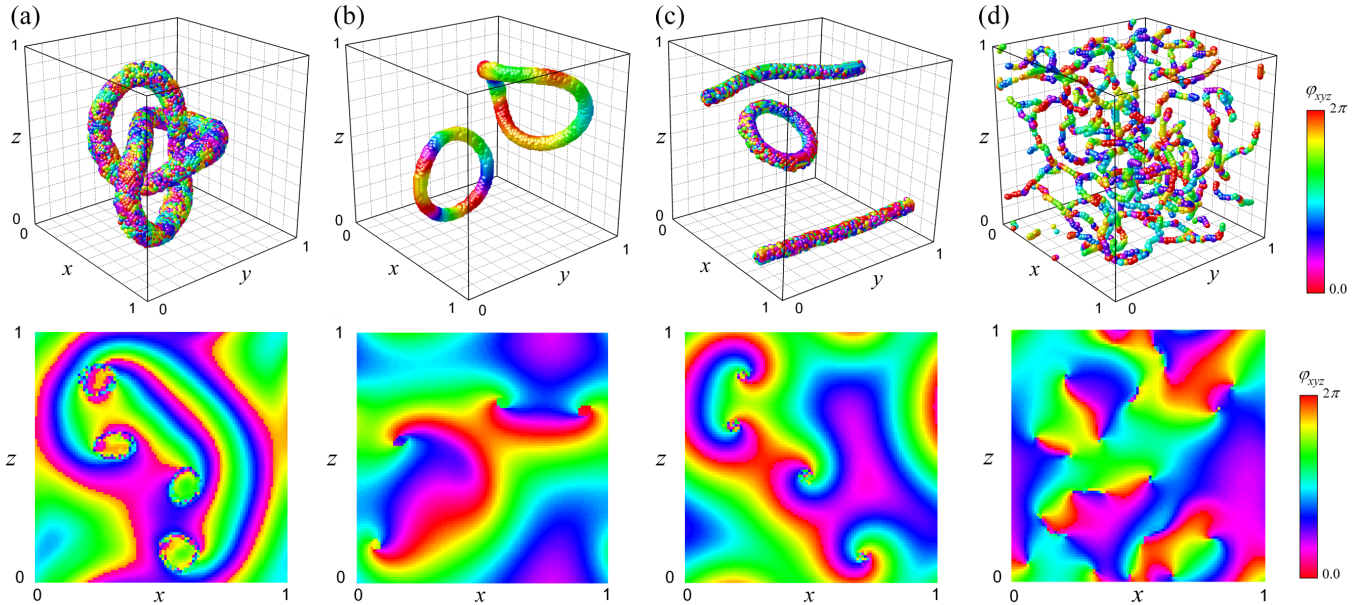


FIG. 5. Scroll wave chimeras in system (1). Phase snapshots and their cross-sections: (a) - trefoil ( $\alpha = 0.35, \epsilon = 0.05, \mu = 0.1, r = 0.03, N = 100$ ); (b) - two rings ( $\alpha = 0.44, r = 0.04, \mu = 0.048, \epsilon = 0.052, N = 100$ ). (c) - ring with two rods ( $\alpha = 0.59, r = 0.055, \mu = 0.01, \epsilon = 0.1, N = 100$ ); (d) - multiple scroll wave chimera ( $\alpha = 0.2, r = 0.02, \mu = 0.1, \epsilon = 0.05, N = 100$ ). Coordinates  $x = i/N, y = j/N, z = k/N$ .

shaped, as typically occurs for chimeras in the Kuramoto model without inertia. Figure 4(b) illustrates the scroll ring chimera with partially coherent inner part and incoherent boundary. In the case of a completely coherent ring (Fig. 4(c)), we have a bistable behavior of oscillators. Their average frequencies  $\bar{\omega}_{xyz}$  are equal to the average frequency of the ring  $\bar{\omega}_{CR}$  or main synchronized cluster  $\bar{\omega}_0$  only. So, it is a scroll ring pattern, but is not scroll ring chimera.

Figure 4 illustrates three average frequency profiles of the inner parts of the scroll rings only. But we suggest that, by increasing the dimension  $N$  of system (1), the different scroll ring structures including multiple stepwise structures similarly to the 2D case [27] can be obtained.

To our surprise, if we take a scroll ring with the coupling radius  $r = 0.041$  and  $\alpha = 0.3$  (yellow point in Fig. 3(b)) and will start to increase the coupling radius  $r$  along the black dashed line, the scroll ring is transformed into a sphere pattern without spiral rotation (shown in the insert in Fig. 3(b)). Approaching the left and bottom boundaries of the stability region of the sphere (Fig. 3(b)), the number of incoherent oscillators on the surface decreases. Finally, the sphere vanishes, by crossing the boundaries of this region. Near the right boundary of the stability region, the sphere becomes an incoherent ball. Just after crossing the right boundary, the ball is transformed firstly into a cube and finally into the pattern consisting of incoherent oscillators with coherent islands which fill all the space except for a narrow coherent layer (shown in the insert in Fig. 3(b)).

In the system without inertia, the scroll wave chimeras have, obviously, incoherent inner parts [15–17]. But, in the system with inertia, as one can see from the phase cross-sections of chimeras in Fig. 5, they may have co-

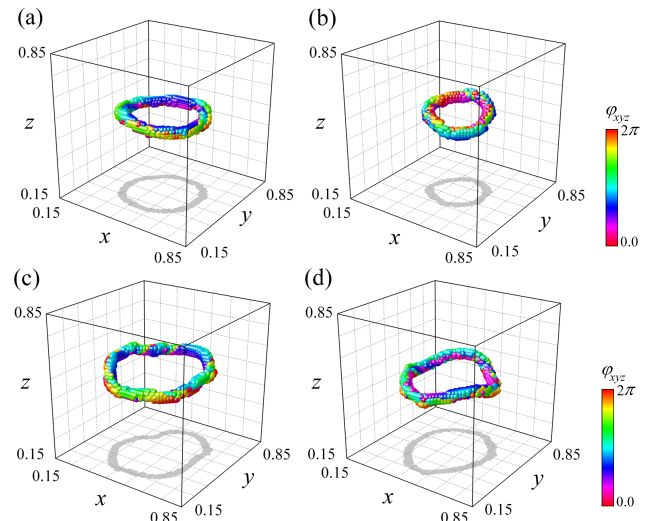


FIG. 6. Perturbated of the scroll ring chimera. (a) - origin scroll ring chimera before perturbation, (b-d) - perturbated scroll ring chimera with amplitude 0.8.  $\alpha = 0.38, r = 0.04, \epsilon = 0.05, \mu = 0.02, N = 100$ . Simulation time  $t = 10^4$ .

herent or partially coherent inner parts. Due to the introduction of the inertia, the trefoil (Fig. 5(a)) and Hopf link chimeras can be fixed in the oscillatory space in contrast to their behavior in a system without inertia, where they move, by rotating around their center of mass.

Scroll wave chimera states from system (1) are very stable with respect to perturbations of the initial conditions. For example, the scroll ring chimera still exists and retains its shape, even if its phase  $\varphi_{xyz}$  and frequency  $\omega_{xyz}$  are perturbed by uniformly distributed noise with amplitude less than 0.5 at the parameter values  $\alpha = 0.38, r = 0.04, \epsilon = 0.05, \mu = 0.02, N = 100$  (yellow point in Fig. 3(a)). Stronger perturbations lead

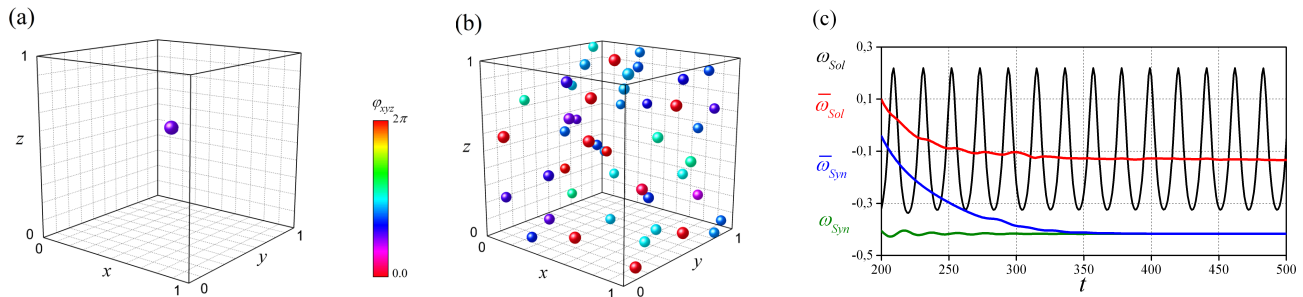


FIG. 7. Solitary states. (a) - phase snapshot for a single solitary state ( $\alpha = 0.21$ ), (b) - phase snapshot for multiple solitary states ( $\alpha = 0.25$ ), (c) - time evolution of frequencies for a single solitary state.  $\mu = 0.1, \epsilon = 0.05, r = 0.04, N = 50$ . Frequency averaging interval  $\Delta T = 200$ . Coordinates  $x = i/N, y = j/N, z = k/N$ .

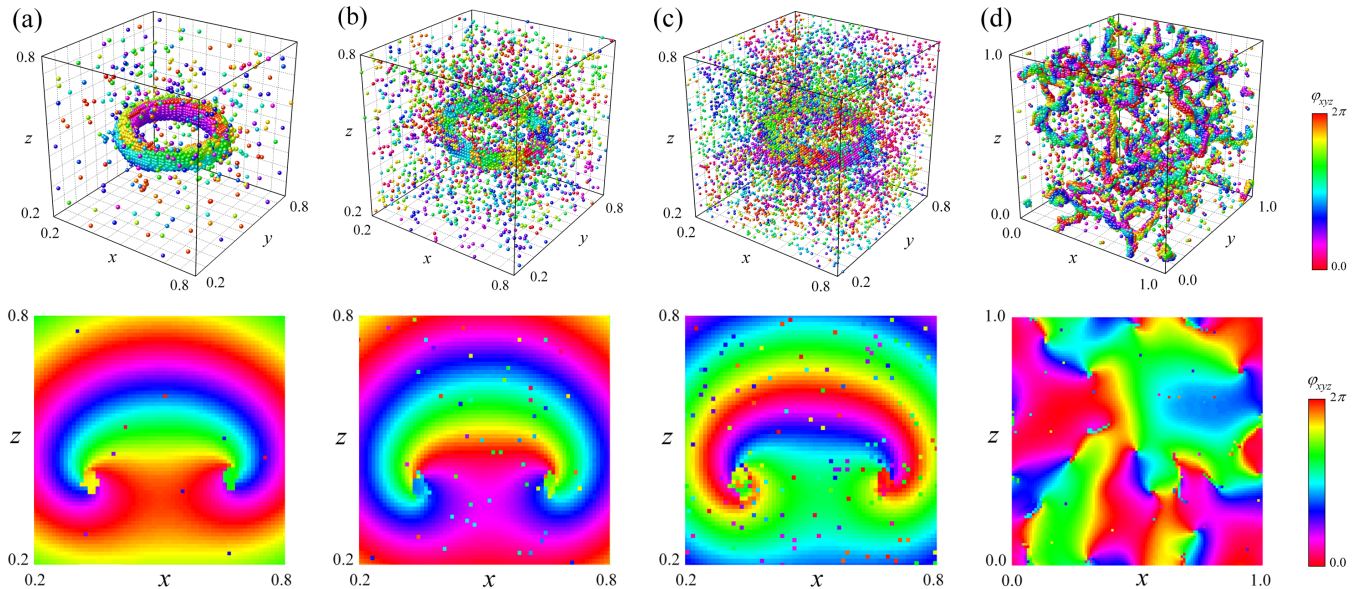


FIG. 8. Examples of the scroll wave chimera states with solitary clouds. Phase snapshots and their cross-sections. Scroll rings chimera perturbed with amplitude: 0.5 (a), 0.55 (b), 0.6 (c) ( $\alpha = 0.4, \mu = 0.1, \epsilon = 0.05, r = 0.03, N = 100$ ). (d) - multiple scroll wave chimera obtained from random initial conditions ( $\alpha = 0.22, \mu = 0.1, \epsilon = 0.05, r = 0.028, N = 100$ ).

to changing the shape of chimeras or its destruction with complete oscillatory synchronization or creation of different types of scroll wave chimera states such as: a few rings, rods, etc. If we take a scroll ring (Fig. 6(a)) outside the solitary region and start to perturb it by uniformly distributed noise with amplitude 0.8, then we can obtain various new scroll ring chimera states with different shapes (Fig. 6(b-d)). So, in this way, we can generate many different rings for fixed parameter values of system (1). For each chimera obtained in this way, we can again apply the perturbation method to generate new scroll ring chimera states and so on.

The dynamics of system (1) becomes more complicated, if the parameter values enter into the solitary region (hatched in gray in Fig. 3) where isolated oscillators exist [25, 26]. Single (Fig. 7(a)) or multiple (Fig. 7(b)) solitary states can be easily obtained from random initial conditions. Multiple solitary states look like a "solitary cloud". An example of the time evolution of frequencies  $\omega_{xyz}$  for a single solitary state from Fig. 7(a) is shown in Fig. 7(c). The frequency of a solitary state  $\omega_{Sol}$  becomes very soon periodic, and its average value  $\bar{\omega}_{Sol}$  tends to a constant. The frequencies of synchronized oscillators

$\omega_{Syn}$  and their average values  $\bar{\omega}_{Syn}$  tend to constants as well. If the disturbed chimera lies in the solitary region, then the perturbation of its initial conditions with amplitude in the interval (0.5 – 0.8) can give rise to another chimera states with solitary clouds. Examples of scroll ring chimeras with solitary clouds are shown in Fig. 8 for the parameter values indicated by the green point in Fig. 3(a). As clearly seen from these figures, the solitary clouds in the oscillatory space can appear with a perturbation of a scroll ring with amplitude 0.5 (Fig. 8(a)). Stronger perturbations with amplitudes 0.55 (Fig. 8(b)) and 0.6 (Fig. 8(c)) save the scroll ring chimera, but clouds becomes denser. The further perturbation of chimera's initial conditions with amplitude more than 0.8 can destroy the original chimera states. We show also multiple scroll wave chimera with solitary clouds (Fig. 8(d)) obtained from random initial conditions.

In such a way, any scroll wave chimera from the solitary region with fixed parameters may have solitary clouds of arbitrary random shape. Such clouds may be obtained by a random perturbation of the original chimera. However, the transition between solitary and non-solitary domains is noninvertible. Perturbations of chimeras with param-

ters outside the solitary regions never lead to the formation of solitary clouds. At the same time, starting from initial conditions with solitary clouds outside the solitary region leads to the vanishing of solitary clouds. On the other hand, starting from initial conditions without solitary cloud inside the solitary region never leads to the formation of a solitary cloud.

Finally, we would like to propose a method of construction of 3D images using solitary states as the solutions of the 3D Kuramoto model with inertia (1). In addition to the image of a chimera sculpture from the Notre-Dame Cathedral (Fig. 1(d)), we present the Eiffel Tower image in Fig. 9 (Multimedia view).

This image is a stable solution of the 3D Kuramoto model with inertia (1). Stable solitary patterns of arbitrary shape may be constructed using dynamic variables of synchronized and solitary oscillators from any other stable solitary state. A model for 3D printing was used as a template for the spatial placing of solitary oscillators.

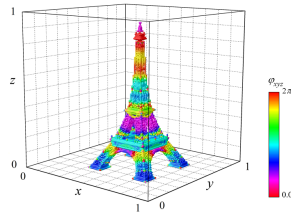


FIG. 9. Phase snapshot of 3D image of the Eiffel Tower as a solution of the 3D system with inertia (1) (Multimedia view).. Parameters  $\alpha = 0.4, r = 0.2, \mu = 0.1, \epsilon = 0.05, N = 200$ .

The 3D Kuramoto model with inertia (1) describes the basic properties of the collective dynamics in various real physical systems. Equations similar to (1) arise in magnonics [30, 31], optics [32], etc. The phenomena similar to chimera and solitary states were observed experimentally in various systems, e.g., with the Josephson effects, Bose–Einstein condensation of magnons [30, 31], pulling of frequencies and optical modes [32], etc. Models of oscillating nonlinear networks are used in biology and electronics. Such properties as the stability of the described chimera and solitary states with respect to perturbations of the initial conditions in a wide range of parameters and the preservation of initial average oscillating frequencies for solitary states may become a key to practical applications.

The practical applications of these phenomena can include the creation of new information storage and transfer media, devices, architectures; development of new information encoding algorithms; clarification of the mechanisms of functioning of biological systems, etc.

The authors are very grateful to Yu. Maistrenko for useful discussions and valuable comments.

**Data availability.** The data that support the findings of this study are available from the corresponding author (maistren@nas.gov.ua) upon reasonable request.

- 
- [1] Y. Kuramoto. *Nonl. Dyn. and Chaos*, CRC Press, pp. 209 – 227, (2002).
- [2] Y. Kuramoto, D. Battogtokh. *Nonlinear Phenom. Complex Syst.* **5**, pp. 380 – 385, (2002).
- [3] D.M. Abrams, S.H. Strogatz. *Phys. Rev. Lett.*, **93**, 174102, (2004).
- [4] Y. Kuramoto, S.I. Shima. *Prog. Theor. Phys. Supp.* **150**, pp.115 – 125, (2003).
- [5] P.-J. Kim, T.-W. Ko, H. Jeong, H.-T. Moon, *Phys. Rev. E* **70**, 065201(R) (2004).
- [6] E. Martens, C. Laing, S. Strogatz. *Phys. Rev. Lett.* **104**, 044101 (2010).
- [7] O.Omel’chenko, M.Wolfrum, S.Yanchuk, Yu.Maistrenko, O.Sudakov. *Phys. Rev. E* **85** (3), 036210, (2012).
- [8] M.J. Panaggio, D.M. Abrams. *Phys. Rev. Lett.* **110**, 094102 (2013).
- [9] J. Xie, E. Knobloch, H.-C. Kao. *Phys. Rev. E.* **92**, 042921 (2015).
- [10] C.R. Laing. *SIAM J. Appl. Dyn. Syst.*, **16**(2), pp. 974 – 1014 (2017).
- [11] O. Omel’chenko, M. Wolfrum, E. Knobloch. *SIAM J. Appl. Dyn. Syst.*, **17**(1), pp. 97 – 127 (2018).
- [12] J.F. Totz, J. Rode, M.R. Tinsley, et al. *Nature Phys.* **14**, pp. 282 – 285 (2018).
- [13] O. Omel’chenko, E. Knobloch. *New Journal of Physics*, **21**, 093034, (2019).
- [14] J.F. Totz. *Spiral Wave Chimera*. In: *Synchronization and Waves in Active Media*, pp.55 - 97. Springer (2019).
- [15] Yu. Maistrenko, O. Sudakov, O. Osiv, V. Maistrenko. *New Journal of Physics*, **17**, 073037, (2015).
- [16] H.W. Lau, J. Davidsen. *Phys. Rev.E*, **94**, 010204(R), (2016).
- [17] V. Maistrenko, O. Sudakov, O. Osiv, Yu. Maistrenko. *EPJ ST*, V. **226**, Issue 9, (2017).
- [18] T. Kasimatis, J. Hizanidis, A. Provata. *Phys. Rev. E* **97**, 052213, (2018).
- [19] S. Kundu, B.K. Bera, B. D. Ghosh, M. Lakshmanan. *Phys. Rev. E*, **99**(2), (2019).
- [20] O.Omel’chenko, E.Knobloch. *New Journal of Physics*, **21**, (2019).
- [21] Yu. Maistrenko, A. Vasylenko, O. Sudakov, R. Levchenko, V. Maistrenko. *Int. J. Bifurc. Chaos.*, **24**, 1440014, (2014).
- [22] A. Winfree. *Science* **181** 937, (1973).
- [23] V. Biktashev, I. Biktasheva. *Engineering of Chemical Complexity II*, pp. 221 - 238, (2014).
- [24] J. Totz, H. Engel, O. Steinbock. *New J. Phys.* **17**, 093043, (2015).
- [25] P. Jaros, Yu. Maistrenko, T. Kapitaniak. *Phys. Rev. E* **91**, 022907, (2015).
- [26] P. Jaros, S. Brezetsky, R. Levchenko, D. Dudkowski, T. Kapitaniak, Yu. Maistrenko. *Chaos* **28**, 011103, (2018).
- [27] V. Maistrenko, O. Sudakov, Yu. Maistrenko. <https://arxiv.org/pdf/2001.02167.pdf>, (2019).
- [28] A. Salnikov, R. Levchenko, O. Sudakov. *Proc. 6th IEEE (IDAACS)*, pp. 198 – 202 (2011).
- [29] O. Sudakov, A. Cherederchuk, V. Maistrenko. *Proc. 9th IEEE (IDAACS)*, pp. 311 - 316 (2017).
- [30] R. Troncoso, Á. Núñez. *Ann. Phys.* **346**, pp.182–194(2014).
- [31] R. Khymyn, I. Lisenkov, V. Tiberkevich, B. Ivanov, A. Slavin. *Sci Rep.* 2017; 7: 43705 (2017).
- [32] A. Fratalocchi, C. Conti, G. Ruocco. *Opt. Express* **16**, pp. 8342–8349 (2008).